Symmetry Driven Irreversibilities at Ferromagnetic-Antiferromagnetic Interfaces

A. Hoffmann

Materials Science Division, Argonne National Laboratory, Argonne, Illinois 60439, USA

(Received 14 January 2004; published 26 August 2004)

The coupling between a ferromagnet and an antiferromagnet can establish a directional anisotropy called exchange bias. In many systems this exchange bias is reduced upon subsequent field cycling, which is referred to as training effects. Numerical simulations of a simple coherent rotation model suggest that the symmetry of the anisotropy in the antiferromagnet is crucial for the understanding of training effects in exchange bias systems. Namely, the existence of multiple antiferromagnetic easy anisotropy axes can initially stabilize a noncollinear arrangement of the antiferromagnetic spins, which relaxes into a collinear arrangement after the first magnetization reversal of the ferromagnet.

DOI: 10.1103/PhysRevLett.93.097203 PACS numbers: 75.70.Cn, 75.60.Ej

Interactions between different magnetic materials in layered systems can give rise to complex magnetic behavior. In particular, the interaction of an antiferromagnet with a ferromagnet can establish a directional coupling, which is referred to as an exchange bias. Even though this effect was first discovered almost 50 years ago [1], the underlying mechanism remains controversial [2–4]. Concurrently, exchange bias has gained technological importance, since it pins and thus establishes a reference magnetization direction in spintronic devices, i.e., in magnetic read heads and nonvolatile memory [5]. Furthermore, many exchange bias systems show an instability which results in a reduction of pinning upon repeated field cycling [6]. These field training effects are suspected to be due to irreversible changes in the magnetic microstructure of the antiferromagnet, but a comprehensive theoretical understanding is still missing. In this Letter a simple and universal model is presented, which implies that the irreversibilities upon field cycling are driven by the symmetry of the anisotropy in the antiferromagnet.

The induced unidirectional anisotropy in antiferromagnetic/ferromagnetic coupled systems generates a shift H_E (exchange bias) of the ferromagnetic hysteresis loop from zero field. In many cases H_E is reduced after the first hysteresis loop. An example of this training effect is shown in Fig. 1 utilizing the historical prototype system Co/CoO. For a 10-nm thick polycrystalline ferromagnetic Co film covered with an antiferromagnetic CoO layer due to ambient oxidation, subsequent hysteresis loops were measured, after the sample was cooled in a field of +5 kOe from 300 to 10 K. This field cooling establishes a shift $H_{E,1}$ in the first hysteresis loop. Furthermore, the first hysteresis loop has a clear overall asymmetry; namely, the first magnetization reversal (with decreasing field) has a sharp jump, while the second reversal (with increasing field) is more gradual. In contrast, the second hysteresis loop is more symmetric, with a significantly smaller shift $H_{E,2}$ and similar shapes for both magnetization reversals. Any subsequent hysteresis loops are essentially unchanged from the second hysteresis loop.

It has been suggested that training effects are connected to the microstructure of exchange bias systems [2,6]. This idea is corroborated by numerical simulations of exchange bias systems with nonmagnetic defects in the antiferromagnet [7]. While these simulations show that the antiferromagnetic spin structure can change after initial field reversal, they fail to show that this leads to successively reduced exchange bias. However, training effects have been observed experimentally in both polycrystalline [1,8] and epitaxial [9–11] systems. More importantly, Malkinski *et al.* have specifically investigated the influence of crystallinity on exchange bias in $Fe/KCoF_3$ [12]. They observed that independent of crystallinity training effects were similar for poly- and single-crystal $KCoF_3$ samples. Moreover, training effects are absent for FeF_2 and MnF_2 based exchange bias sys-

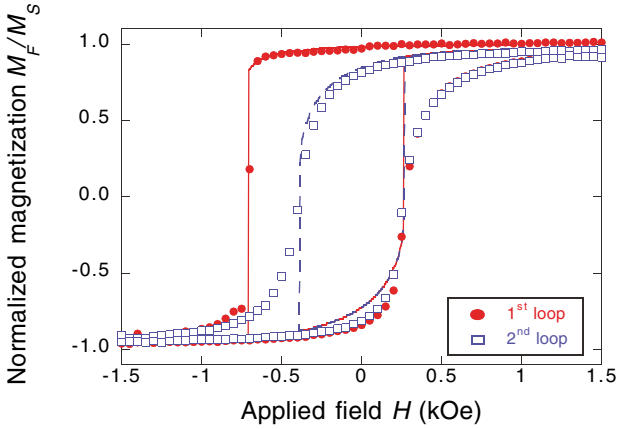

FIG. 1 (color online). Field dependence of the magnetization of a polycrystalline Co/CoO bilayer showing the first (solid symbols) and second (open symbols) hysteresis loop after field cooling. The magnetization M_F is normalized by the saturation value M_S. The solid and dashed lines show calculated hysteresis loops for comparison [22].

 0031-9007/04/93(9)/097203(4)$22.50

tems independent of crystalline structure [13]. This suggests that microstructure is not the critical parameter for training effects.

A list of antiferromagnets sorted by the occurrence of training effects in exchange bias systems is shown in Table I. Note that all exchange bias systems where training effects occur contain high symmetry antiferromagnets with multiple equivalent easy magnetic axes. In contrast, systems where training effects are absent for a wide variety of different samples contain only antiferromagnets with uniaxial magnetic anisotropy. This is the first clue that the symmetry of the magnetic anisotropy in the antiferromagnet is crucial to understand training effects.

Numerical simulations of magnetic hysteresis curves for exchange bias systems with different symmetries for the antiferromagnet are presented below to further explore this interesting clue. Using two independent magnetic sublattices for the antiferromagnet [20], one can write the energy of the exchange bias system in a coherent rotation model [21] as

$$E = -\mathbf{H}\cdot\mathbf{M_F} - J_I\mathbf{M_F}\cdot\sum_{i=A,B}\mathbf{M_i} - \mathbf{H}\cdot\sum_{i=A,B}\mathbf{M_i} - J_{\mathrm{AF}}\mathbf{M_A}\cdot\mathbf{M_B} + E_K(\mathbf{M_A},\mathbf{M_B}), \quad (1)$$

where $\mathbf{H}$ is the external magnetic field, $\mathbf{M_F}$ is the magnetization of the ferromagnet, $\mathbf{M_A}$ and $\mathbf{M_B}$ are the two antiferromagnetic sublattice magnetizations, J_I is the coupling between the ferromagnet and each antiferromagnetic sublattice, and $J_{\mathrm{AF}} < 0$ is the antiferromagnetic coupling between the two antiferromagnetic sublattices within the antiferromagnet. Notice that the second term in Eq. (1) couples the ferromagnet to both antiferromagnetic sublattices. This is consistent with either a spin-compensated surface of the antiferromagnet or a spin-uncompensated surface with significant interface roughness [4]. The last term in Eq. (1), E_K, is the anisotropy energy of the antiferromagnet given by either

$$E_K = KM_{\mathrm{AF}}[\sin^2(2\phi_A) + \sin^2(2\phi_B)] \quad \text{or} \quad (2a)$$

$$E_K = KM_{\mathrm{AF}}[\sin^2(\phi_A) + \sin^2(\phi_B)] \quad (2b)$$

for the case of biaxial (2a) or uniaxial (2b) symmetry of the anisotropy. K is the anisotropy constant, $M_{\mathrm{AF}} = |\mathbf{M_A}| = |\mathbf{M_B}|$, and ϕ_A and ϕ_B are the angles between one of the easy-axis directions and each antiferromagnetic sublattice magnetization. In this model it is assumed that all magnetizations and anisotropies are confined within the plane of the interface.

Using Eq. (1), magnetic hysteresis loops can be calculated by energy minimization as a function of applied field H. The starting point for the first hysteresis loop is the global energy minimum for the initial magnetic field. This assumes that during the field-cooling process there is enough thermal energy for the system to relax to the lowest energy state. Figure 2 shows the simulated hysteresis loops for biaxial [Fig. 2(a)] and uniaxial [Fig. 2(b)] anisotropy. The blue solid line shows the first hysteresis loop, while the second one is shown by a red dashed line. The parameters for both cases are $|\mathbf{M_F}| = |\mathbf{M_A}| + |\mathbf{M_B}|$, $J_I = -J_{\mathrm{AF}}$, $K = -0.4J_{\mathrm{AF}}M_{\mathrm{AF}}$, and the field direction is 20° with respect to one of the easy axes. The result is very striking; while the biaxial symmetry case shows clear training effects, reproducing important features of the experimental data as discussed below, the simulation with uniaxial symmetry shows no difference between the first and second hysteresis loops. Similar results are obtained for other orientations of the easy axes and other values for the anisotropy or interface coupling. It should be noticed that a net exchange bias for the unixaial case or after training can be reproduced, if an imbalance between the two antiferroamgnetic sublattice magnetizations is assumed [4,22] (see also Fig. 1). For

TABLE I. Antiferromagnets of exchange-biased systems.

Training observed	No training observed
CoO[a]	FeF_2[b]
FeO[c]	MnF_2[d]
FeMn[e]	
$Ir_{22}Mn_{78}$[f]	
$KCoF_3$[g]	
NiFeMn[h]	
NiO[i]	
PtPdMn[j]	

[a]From Refs. [6,8,9].
[b]From Ref. [14].
[c]From Ref. [15].
[d]From Refs. [14,16].
[e]From Ref. [17].
[f]From Ref. [18].
[g]From Ref. [12].
[h]From Ref. [6].
[i]From Refs. [10,11].
[j]From Ref. [19].

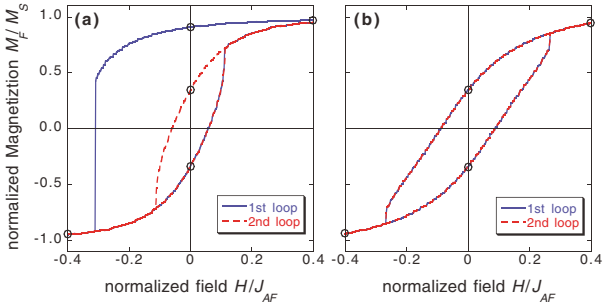

FIG. 2 (color online). Calculated hysteresis loops. (a) Biaxial anisotropy of the antiferromagnet; (b) uniaxial anisotropy. Shown are the first (solid line) and the second (dashed line) hysteresis loop, which are in the case of uniaxial anisotropy (b) identical. The circles indicate the fields for which the relative orientation of the different magnetizations is shown in Fig. 3.

example, such an imbalance may be caused by a domain structure within the antiferromagnet [7].

Figure 3 shows the orientation of the various magnetizations close to saturation and in remanence during all of the first and half of the second hysteresis cycle. In the uniaxial case (lower row) the sublattice magnetizations are always essentially antiparallel and along the easy axis. However, in the biaxial case (upper row) the antiferromagnetic sublattice magnetizations are initially perpendicular. Only after the first field reversal do the antiferromagnetic sublattices relax into an antiparallel arrangement. Immediately the question arises: Why are the antiferromagnetic sublattices initially perpendicular in the biaxial case? Because of the coupling of both antiferromagnetic sublattices to the ferromagnet there is an inherent frustration, similar to that found in geometrically frustrated magnets [23]. The antiferromagnetic coupling J_{AF} prefers an antiparallel orientation of the two antiferromagnetic sublattices, while the interfacial coupling J_I of each of the sublattices to the ferromagnetic magnetization favors a parallel orientation of the two sublattices, irrespective of the sign of J_I. When J_I is comparable to J_{AF}, this frustration results in energetically favoring a perpendicular configuration of the antiferromagnetic sublattices. However, after the ferromagnetic magnetization is reversed, the initial perpendicular arrangement no longer reduces the frustration, and the antiferromagnet then relaxes into a metastable anti-

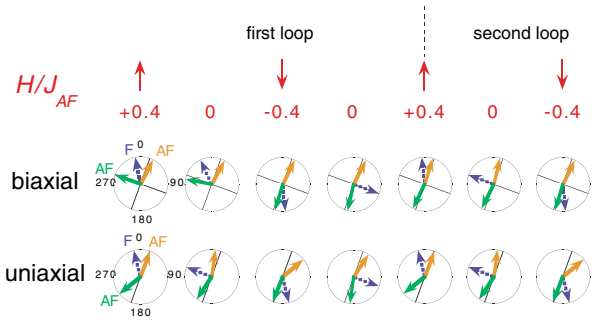

FIG. 3 (color online). Orientation of magnetizations. Shown are the ferromagnetic (dashed arrow) and each antiferromagnetic sublattice magnetization (solid arrows) for saturation and remanence during the first and half of the second hysteresis loop. The solid lines indicate the directions of the antiferromagnetic anisotropy axes.

parallel configuration where it remains for subsequent hysteresis loops. Only the application of a large field exceeding the spin-flop field of the antiferromagnet would recover the original perpendicular sublattice configuration.

One important question is this: How sensitively does the initial perpendicular arrangement depend on the model parameters? For large biaxial anisotropy one can determine the different lowest energy states as a function of orientation ϕ of the easy axis with the cooling field H_C. One can distinguish three cases:

$$0 < \left| \frac{J_I M_F + H_C}{J_{\mathrm{AF}} M_{\mathrm{AF}}} \right| < \frac{1}{\cos(\phi) + \sin(\phi)}, \tag{3a}$$

$$\frac{1}{\cos(\phi) + \sin(\phi)} < \left| \frac{J_I M_F + H_C}{J_{\mathrm{AF}} M_{\mathrm{AF}}} \right| < \frac{1 - \frac{2K \sin^2(2\phi)}{J_{\mathrm{AF}} M_{\mathrm{AF}}}}{2 - \cos(\phi) - \sin(\phi)}, \quad \text{and} \tag{3b}$$

$$\frac{1 - \frac{2K \sin^2(2\phi)}{J_{\mathrm{AF}} M_{\mathrm{AF}}}}{2 - \cos(\phi) - \sin(\phi)} < \left| \frac{J_I M_F + H_C}{J_{\mathrm{AF}} M_{\mathrm{AF}}} \right|. \tag{3c}$$

For the case (3a) the global minimum occurs at the antiparallel configuration, for (3b) the perpendicular configuration is stable, and for (3c) the coupling of the antiferromagnet to the ferromagnet and the cooling field H_C becomes strong enough to align the antiferromagnetic sublattices. Only the boundary between (3b) and (3c) is explicitly dependent on the magnitude of the anisotropy (and is depicted in Fig. 4 for $K = -0.4 J_{\mathrm{AF}} M_{\mathrm{AF}}$). A wide range of parameters support the perpendicular configuration as the global free energy minimum (see Fig. 4). Notice also that even for very small values of K there is still a large range of parameters that favor the perpendicular orientation, namely, $|J_I M_F + H_C| \approx |J_{\mathrm{AF}} M_{\mathrm{AF}}|$. This is consistent with the fact that experimentally training effects are observed in diverse exchange bias systems.

A comparison between experimental data (Fig. 1) and the simulated hysteresis loop (Fig. 2) shows that the model reproduces several distinct features, namely, the sharp jump at the first magnetization reversal and the overall more symmetric second hysteresis loop. Even better agreement between the experimental data and the simulated hysteresis loops can be achieved by adding an anisotropy parameter to describe the ferromagnet. Room temperature measurements of the aforementioned Co/CoO sample reveal a uniaxial anisotropy field. Including such an uniaxial anisotropy in the numerical simulation gives rise to hysteresis loops, which reproduce main features of the experimental data surprisingly well (see Fig. 1).

Neutron scattering from Co/CoO bilayers [8] has shown that during the first reversal the Co layer develops domains that are parallel or antiparallel to the applied field, while in subsequent reversals the magnetization rotates mostly perpendicular to the applied field. Similar behavior is observed in the simulated hysteresis loops. During the first reversal, the ferromagnetic magnetization

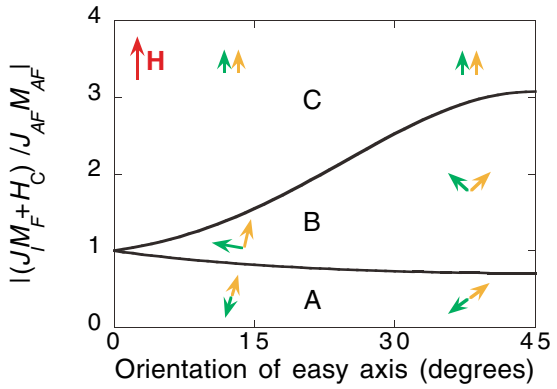

FIG. 4 (color online). Phase diagram for initial configuration of the antiferromagnetic sublattices after field cooling. For the case of ferromagnetic interfacial coupling ($J_{\mathrm{Int}} > 0$), the arrows indicate symbolically the orientations of the antiferromagnetic sublattices with respect to the applied magnetic field **H** (represented by an arrow in the top left corner).

remains almost antiparallel to the applied field, stabilized by the net moment of the perpendicular configuration of the antiferromagnetic sublattices. The relaxation of the antiferromagnet into an antiparallel configuration, after the ferromagnetic magnetization switches, results in an easy axis for the ferromagnet that is perpendicular to the antiferromagnetic sublattices due to spin-flop coupling [24]. Thus, after the first reversal, the resulting ferromagnetic easy axis is within $90 \pm 45°$ with respect to the applied field.

Generally, training effects are most pronounced for thin antiferromagnetic layers [10,19]. The role of the antiferromagnet thickness becomes clear by looking at the phase diagram in Fig. 4. With increasing antiferromagnet thickness, $J_{\mathrm{AF}} M_{\mathrm{AF}}$ dominates over $J_I M_F$, and the initial perpendicular arrangement of the antiferromagnetic sublattices, which is necessary for the training effects, is no longer energetically favorable.

It has been suggested that training effects are more common for polycrystalline samples compared to single crystalline antiferromagnets [2]. Again, the phase diagram in Fig. 4 can explain this. Depending on the ratio $|(J_I M_F + H_C)/J_{\mathrm{AF}} M_{\mathrm{AF}}|$, the direction of the magnetic field will determine the presence of training effects. Thus more careful investigations of training effects as a function of magnetic field orientation should be undertaken for epitaxial systems.

The calculations presented in this work show that irreversible training effects in exchange coupled antiferromagnetic/ferromagnetic systems may be determined by the inherent frustration of the interface and the symmetry of the antiferromagnetic anisotropies. Therefore it should inspire further investigations of irreversible effects and thus enable a better understanding of the role of symmetry in the coupling of magnetic heterostructures.

This work was inspired by questions from Ivan K. Schuller and benefited from many useful discussions with S. D. Bader, M. Grimsditch, J. Meersschaut, T. Schulthess, and H. Suhl. The work was supported by the Office of Basic Energy Sciences, U.S. Department of Energy, under Contract No. W-31-109-ENG-38.

[1] W. H. Meiklejohn and C. P. Bean, Phys. Rev. **102**, 1413 (1956).
[2] J. Nogués and I. K. Schuller, J. Magn. Magn. Mater. **192**, 203 (1999).
[3] A. E. Berkowitz and K. Takano, J. Magn. Magn. Mater. **200**, 552 (1999).
[4] M. Kiwi, J. Magn. Magn. Mater. **234**, 584 (2001).
[5] J. C. S. Kools, IEEE Trans. Magn. **32**, 3165 (1996).
[6] D. Paccard, C. Schlenker, O. Massenet, R. Montmory, and A. Yelon, Phys. Status Solidi **16**, 301 (1966).
[7] U. Nowak, K. D. Usadel, J. Keller, P. Miltényi, B. Beschoten, and G. Güntherodt, Phys. Rev. B **66**, 014430 (2002).
[8] W. T. Lee, S. G. E. te Velthuis, G. P. Felcher, F. Klose, T. Gredig, and E. D. Dahlberg, Phys. Rev. B **65**, 224417 (2002).
[9] J. Keller, P. Miltényi, B. Beschoten, G. Güntherodt, U. Nowak, and K. D. Usadel, Phys. Rev. B **66**, 014431 (2002).
[10] C.-H. Lai, H. Matsuyama, R. L. White, T. C. Anthony, and G. G. Bush, J. Appl. Phys. **79**, 6389 (1996).
[11] A. Hochstrat, C. Binek, and W. Kleemann, Phys. Rev. B **66**, 092409 (2002).
[12] L. Malkinski, T. O'Keevan, R. E. Camley, Z. Celinski, L. Wee, R. L. Stamps, and D. Skrzypek, J. Appl. Phys. **93**, 6835 (2003).
[13] M. R. Fitzsimmons *et al.*, Phys. Rev. B **65**, 134436 (2002).
[14] M. R. Fitzsimmons, P. Yashar, C. Leighton, I. K. Schuller, J. Nogués, C. F. Majkrzak, and J. A. Dura, Phys. Rev. Lett. **84**, 3986 (2000).
[15] Y. J. Chen, D. K. Lottis, E. D. Dahlberg, J. N. Kuznia, A. M. Wowchak, and P. I. Cohen, J. Appl. Phys. **69**, 4523 (1991).
[16] I. N. Krivorotov, C. Leighton, J. Nogués, I. K. Schuller, and E. D. Dahlberg, Phys. Rev. B **65**, 100402(R) (2002).
[17] C. Schlenker, S. S. P. Parkin, J. C. Scott, and K. Howard, J. Magn. Magn. Mater. **54–57**, 801 (1986).
[18] H. Xi and R. M. White, Phys. Rev. B **64**, 184416 (2001).
[19] C.-Y. Hung, M. Mao, S. Funeda, T. Schneider, L. Miloslavsky, M. Miller, C. Qian, and H.-C. Tong, J. Appl. Phys. **87**, 4915 (2000).
[20] T. Nagamiya, K. Yosida, and R. Kubo, Adv. Phys. **4**, 1 (1955).
[21] E. C. Stoner and E. P. Wohlfarth, Philos. Trans. R. Soc. London A **240**, 599 (1948).
[22] The parameters for the numerical simulation in Fig. 1 are $|\mathbf{M_F}| = |\mathbf{M_A}| + |\mathbf{M_B}|, |\mathbf{M_A}|/|\mathbf{M_B}| = 1.08$, $J_I = -0.8 J_{\mathrm{AF}}$, $K_{\mathrm{AF}} = -0.36 J_{\mathrm{AF}} M_{\mathrm{AF}}$, and $K_F = 0.08 J_I M_F$. The easy axes of the antiferromagnetic and ferromagnetic anisotropies are with respect to the applied field at 50° and 30°, respectively.
[23] A. P. Ramirez, Czech. J. Phys. **46**, Suppl. S6, 3247 (1996).
[24] N. C. Koon, Phys. Rev. Lett. **78**, 4865 (1997).